MACHINE TOOL VOLUMETRIC ERROR MODELING METHOD BASED ON CONTINUOUS-TIME DYNAMIC COMPENSATION

Wenwen DING[1], Yongwen HU[2*], Xiuqin ZHANG[2], Guohua CHEN[2,3], Bo ZHOU[2,3]

Traditional methods for compensating machine tools' volumetric error rely on discrete position data, resulting in intermittent correction effects and residual systematic errors due to insufficient consideration of the Abbe/Bryan principles. To address these issues, this study proposed a continuous-time-based dynamic compensation method. Firstly, a volumetric error model integrating Abbe and Bryan offsets was constructed and simplified by converting Bryan point coordinates to Abbe points, resolving errors introduced by principle-based deviations during measurement. Secondly, a continuous-time dynamic compensation model was developed using the Matlab/Simulink platform, which generated continuous position signals through speed-time integration to achieve real-time correction of full-stroke errors, overcoming the intermittent defects of discrete compensation.Verification on the XHK715 3-axis machining center showed significant dynamic compensation effects: the linear profile deviation decreased from 0.1677 mm before compensation to 0.0507 mm, with surface roughness improved by over 40%. Compared with static error compensation, the maximum positioning errors of three axes decreased from 6.82 μm, 9.80 μm, and 13.49 μm to 4.14 μm, 4.83 μm, and 5.66 μm respectively; the maximum straightness errors were optimized from -8.63 μm, -13.78 μm, and -10.29 μm to -4.26 μm, -5.11 μm, and 4.68 μm ; the maximum angular errors were improved from -15.27 μrad, 6.35 μrad, and 16.69 μrad to 5.31 μrad, 3.64 μrad, and 6.38 μrad . The error stability of each axis is improved by over 60%. This method effectively enhanced machining accuracy and stability, providing a reliable technical solution for the precision upgrade of high-end CNC machine tools.

Keywords: volumetric error compensation; Abbe and Bryan principles; continuous-time dynamic compensation; Matlab/Simulink Modeling

1. Introduction

In modern advanced manufacturing, the machine tools' machining accuracy directly determines the performance and reliability of high-end

* Corresponding author
1 Science and Technology College of Hubei University of Arts and Science, Xiangyang, China.
2 Hubei University of Arts and Science, Xiangyang, China.
3 Xiangyang Key Laboratory of Precision Manufacturing and Special Processing, Xiangyang, China.
Email: 117610811@qq.com

equipment, with volumetric error compensation technology being one of the core means to improve accuracy [1]. Currently, many scholars proposed various modeling methods, among which Homogeneous Transformation Matrix (HTM) is widely used mathematical tools in CNC machine tool modeling. It has been the mainstream method for global error analysis since the 2010s [2]. Although HTM kinematic models have limitations in inverse kinematic solutions and computational efficiency[3], screw theory[4] has attracted attention in recent years due to its higher computational efficiency. Additionally, modeling methods such as the D-H method[5], Multi-Body System (MBS) theory[6], machine learning technology, trigonometric functions, and vector expressions [7] are relatively mature.

Traditional volumetric error compensation methods take discrete position coordinates (such as axis positions measured by encoders) as input and achieve error correction through piecewise interpolation. However, this compensation mode based on discrete points has inherent flaws: in high-speed feeding or complex trajectory machining, errors between adjacent sampling points cannot be corrected in real-time, leading to intermittent fluctuations in compensation effects. Microscopic accuracy losses are particularly likely to occur in curved surface contour machining [8]. This discrete compensation defect has become a key bottleneck restricting further improvements in the high-end machine tools' accuracy .

At the same time, existing error modeling often ignores the fundamental impact of measurement principles on compensation accuracy. As basic criteria for precision measurement, the Abbe principle and Bryan principle clearly state that when the axis to measure is not collinear with the measured axis, angular errors will introduce Abbe offset errors (linear errors) and Bryan offset errors (straightness errors) respectively [9]. However, most machine tool error measurements are limited by equipment installation space (such as placing instruments on the worktable), making it difficult to meet these two principles, resulting in systematic deviations mixed into the measurement data. Even with high-precision sensors, there are still residual errors that are difficult to eliminate after compensation, which is particularly prominent in ultra-precision machining of aerospace parts [10].

Currently, academic circles have proposed modeling methods such as homogeneous transformation matrices and multi-body system theory, but these methods mostly focus on the completeness of mathematical expressions and insufficiently integrate Abbe/Bryan errors [11]; commercial CNC systems generally adopt quasi-static compensation strategies that rely on discrete position data and cannot achieve continuous dynamic correction[12]. Therefore, addressing the limitations of discrete compensation while systematically incorporating fundamental measurement principles into error modeling has become a pressing

challenge for enhancing the effectiveness of volumetric error compensation in machine tools.

For the above issues, a continuous-time-based dynamic compensation method for machine tool volumetric errors was proposed: Firstly, a geometric model characterizing volumetric deviations was given with Abbe principles Subsequently, coordinate transformation was employed to streamline the model, thereby addressing the oversight of principle-related errors inherent in conventional modeling approaches. Secondly, the Matlab/Simulink platform was used to build a continuous-time dynamic compensation model, which realized real-time correction of full-stroke errors based on time to overcome the intermittent defects of discrete compensation. Finally, the effectiveness was verified through machining experiments on the XHK715 3-axis machining center. This research seeks to offer a more precise and stable error compensation solution for high-end CNC machine tools, while enhancing the competitiveness of domestic equipment in the realm of precision manufacturing.

2 Volumetric error modeling for 3-axis CNC machines grounded in Abbe and Bryan's principles

2.1 Coordinate-Space Representation of Abbe and Bryan Principles in CNC Systems

In 1890, Ernst Abbe proposed that Abbe error occurs during linear measurements when the axes of the measurement system and the measured workpiece displacement are not aligned, and when there are angular errors in the positioning system. From Fig. 1, when the tool is cutting, it's center point (TCP) is not co-linear with the machine axis where the measurement reference point is located.

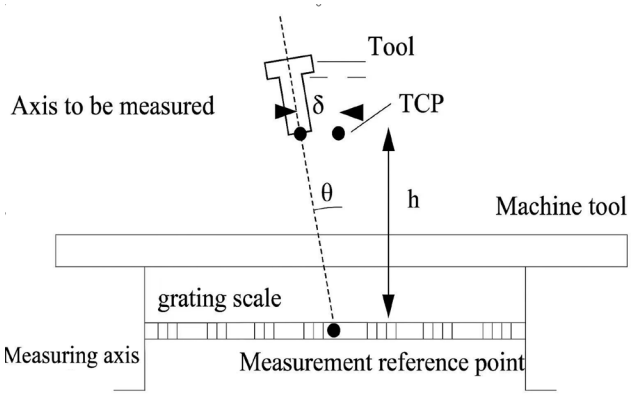

Fig. 1. Diagram of Abbe error.

There is an Abbe height offset (h) between the two axes, and an angular error (θ) during motion causes a deviation in the TCP, i.e., Abbe error ($\delta = h\theta$). Similarly

to the Abbe principle, according to the Bryan principle, when straightness errors are detected in the same manner, the actual measurement axis does not coincide with the axis to be measured, resulting in a Bryan offset between the two axes. The angular error introduces a Bryan error in the measured straightness error.

2.2 Volumetric error modeling for 3-axis CNC machines

In actual machine tool applications, Abbe and Bryan errors occur along the three axes, and each error must be compensated individually. As shown in Fig. 2, based on these principles, the reference position refers to Abbe point and th straightness points refers to the Bryan point[13].

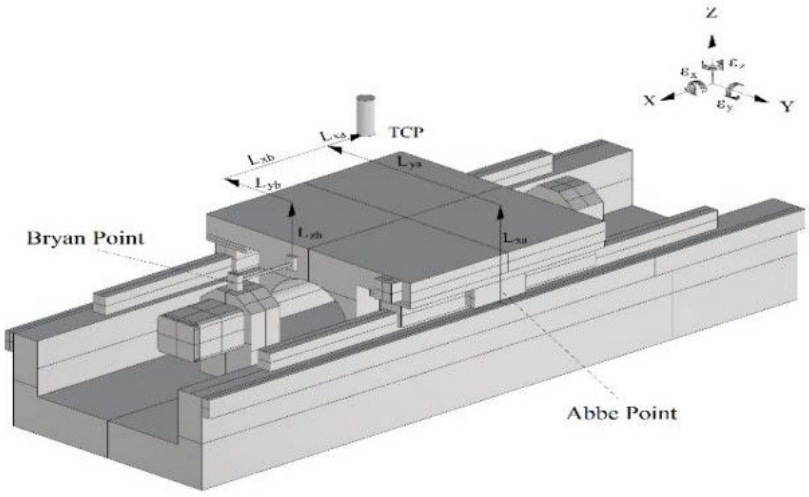

Fig. 2. TCP position error generated by Abbe and Bryan principles.

From the TCP to the Abbe point, there are three directions of Abbe offsets (Lxa, Lya, Lza). Similarly, there are three directions of Bryan offsets (Lxb, Lyb, Lzb) from the Bryan point to the TCP, along with the volumetric error component caused by squareness. The volumetric error for each axis at the TCP is determined using the following formula:

$$E_x(x) = \delta_{xa}(x) - \varepsilon_z(x)L_{ya}(x) + \varepsilon_y(x)L_{za}(x) - (S_{xy} \cdot Y + S_{xz} \cdot Z) \quad (1)$$

$$E_y(x) = \delta_{yb}(x) + \varepsilon_x(x)L_{xb}(x) - \varepsilon_x(x)L_{zb}(x) \quad (2)$$

$$E_z(x) = \delta_{zb}(x) - \varepsilon_y(x)L_{xb}(x) + \varepsilon_x(x)L_{yb}(x) \quad (3)$$

For Y-axis:

$$E_x(y) = \delta_{xb}(y) + \varepsilon_y(y)L_{zb}(y) - \varepsilon_z(y)L_{yb}(y) \quad (4)$$

$$E_y(y) = \delta_{ya}(y) + \varepsilon_z(y)L_{xa}(y) - \varepsilon_x(y)L_{za}(y) - S_{yz} \cdot Z \quad (5)$$

$$E_z(y) = \delta_{zb}(y) + \varepsilon_x(y)L_{yb}(y) - \varepsilon_y(y)L_{xb}(y) \quad (6)$$

For Z-axis:

$$E_x(z) = \delta_{zb}(z) + \varepsilon_y(z)L_{zb}(z) - \varepsilon_z(z)L_{yb}(z) \quad (7)$$

$$E_y(z) = \delta_{yb}(z) + \varepsilon_z(z)L_{xb}(z) - \varepsilon_x(z)L_{zb}(z) \quad (8)$$

$$E_z(z) = \delta_{za}(z) + \varepsilon_x(z)L_{ya}(z) - \varepsilon_y(z)L_{xa}(z) \quad (9)$$

2.3 Model simplifications

Eqs. 1–9 respectively include Abbe and Bryan offsets. For the purpose of simplification, the Abbe and Bryan offsets are unified by transforming the straightness reference from the Bryan point to the Abbe point, thereby ensuring that all linearity errors are consistently defined relative to the Abbe reference. From Fig. 3, the positions of these two points are fixed, with the relative distances denoted as $\Delta L_x, \Delta L_y, \Delta L_z$.

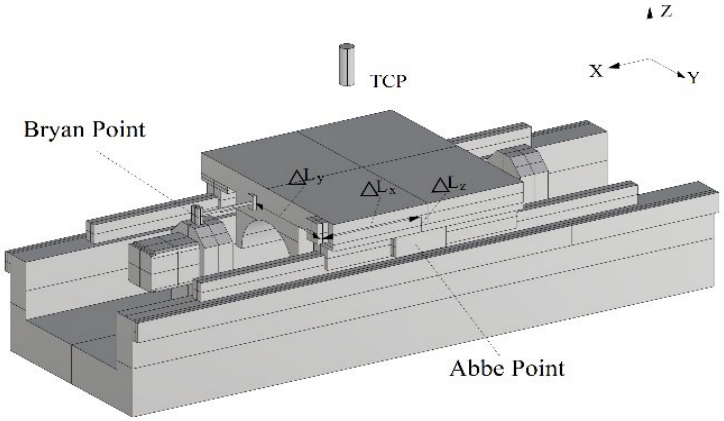

Fig. 3. Geometric Displacement Between Abbe and Bryan Points

The reference linearity error, after being mapped from the Bryan coordinate to the Abbe point, is defined as follows:

In the X-axis direction:

$$\delta_{ya}(x) = \delta_{yb}(x) + \varepsilon_z(x)\Delta L_x(x) - \varepsilon_x(x)\Delta L_z(x) \quad (10)$$

$$\delta_{za}(x) = \delta_{zb}(x) - \varepsilon_y(x)\Delta L_x(x) + \varepsilon_x(x)\Delta L_y(x) \quad (11)$$

In the Y-axis direction:

$$\delta_{xa}(y) = \delta_{xb}(y) + \varepsilon_y(y)\Delta L_z(y) - \varepsilon_z(y)\Delta L_y(y) \quad (12)$$

$$\delta_{za}(y) = \delta_{zb}(y) - \varepsilon_y(y)\Delta L_x(y) + \varepsilon_x(y)\Delta L_y(y) \quad (13)$$

In the Z-axis direction:

$$\delta_{xa}(z) = \delta_{xb}(z) - \varepsilon_z(z)\Delta L_y(z) + \varepsilon_y(z)\Delta L_z(z) \quad (14)$$

$$\delta_{ya}(z) = \delta_{yb}(z) - \varepsilon_x(z)\Delta L_z(z) + \varepsilon_z(z)\Delta L_x(z) \quad (15)$$

As shown in Figure 3, the Abbe points along machine tools' three axes are denoted as X_a, Y_a, Z_a, respectively. Figure 3 depicts the Abbe offsets along each coordinate axis from the Abbe reference point to the tool center point (TCP). For the X-axis motion, the corresponding offsets are denoted as $L_{x(x)}$ in the X-direction, $L_{y(x)}$ in the Y-direction, and $L_{z(x)}$ in the Z-direction. The subscript refers to the direction of the offset, while the bracket indicates the orientation of the moving axis. The same applies to the other two axes. As the X-axis is traversed, the positioning deviation at the corresponding Abbe point is expressed

as $\delta_{xa}(x)$, while the straightness deviations in the Y and Z directions are represented by $\delta_{ya}(x)$ and $\delta_{za}(x)$, respectively. Equivalent relationships are defined for the Y- and Z-axis movements.

Therefore, Eqs. (1)–(9) can be simplified as follows:

For X-axis:

$$E_x(x) = \delta_{xa}(x) - \varepsilon_z(x)L_y(x) + \varepsilon_y(x)L_z(x) - (S_{xy} \cdot Y + S_{xz} \cdot Z) \quad (16)$$

$$E_y(x) = \delta_{ya}(x) + \varepsilon_z(x)L_x(x) - \varepsilon_x(x)L_z(x) \quad (17)$$

$$E_z(x) = \delta_{za}(x) - \varepsilon_y(x)L_x(x) + \varepsilon_x(x)L_y(x) \quad (18)$$

For Y-axis:

$$E_x(y) = \delta_{xa}(y) + \varepsilon_y(y)L_z(y) - \varepsilon_z(y)L_y(y) \quad (19)$$

$$E_y(y) = \delta_{ya}(y) + \varepsilon_z(y)L_x(y) - \varepsilon_x(y)L_z(y) - S_{yz} \cdot Z \quad (20)$$

$$E_z(y) = \delta_{za}(y) + \varepsilon_x(y)L_y(y) - \varepsilon_y(y)L_x(y) \quad (21)$$

For Z-axis:

$$E_x(z) = \delta_{xa}(z) + \varepsilon_y(z)L_z(z) - \varepsilon_z(z)L_y(z) \quad (22)$$

$$E_y(z) = \delta_{ya}(z) + \varepsilon_z(z)L_x(z) - \varepsilon_x(z)L_z(z) \quad (23)$$

$$E_z(z) = \delta_{za}(z) + \varepsilon_x(z)L_y(z) - \varepsilon_y(z)L_x(z) \quad (24)$$

This type of machine tools' volumetric error model simplified according to the Abbe and Bryan principles, is the sum of each axis' error components, as expressed by the following equation:

$$E_x = E_x(x) + E_x(y) + E_x(z) \quad (25)$$

$$E_y = E_y(x) + E_y(y) + E_y(z) \quad (26)$$

$$E_z = E_z(x) + E_z(y) + E_z(z) \quad (27)$$

Notably, as the tool is installed on the spindle and rigidly attached to the Z-axis, the spatial offset between the TCP and the Abbe reference along the Z-axis remains invariant during machine operation. However, the offsets between the TCP and the Abbe references along the X- and Y-axes vary with the machine's motion and are therefore not constant; they vary with the movement of the machine tool. Therefore, under motion conditions, the offsets between the TCP and the Abbe points on each axis of the machine are shown in Table 1. In the table, the right subscript 0 denotes the initial offset between the TCP and the Abbe points when the machine is positioned at the absolute zero point.

Table 1

The styles defined in the IOSPressDoubleColumnJournal.dot file

X-axis	Y-axis	Z-axis
$L_x(x) = L_{x0}(x) - x$	$L_x(y) = L_{x0}(y)$	$L_x(z) = L_{x0}(z)$
$L_y(x) = L_{y0}(x) -$	$L_y(y) = L_{y0}(x) -$	$L_y(z) = L_{y0}(z)$
$L_z(x) = L_{z0}(x) +$	$L_z(y) = L_{z0}(y) +$	$L_z(z) = L_{z0}(z)$

3 Dynamic compensation of machine quasi-static errors based on continuous time

3.1Modeling principles and processes

Matlab/Simulink is based on matrix computations and integrates mathematical calculations, data visualization, and system simulation, enabling functions such as engineering analysis, algorithm development, and mathematical modeling and simulation. The simulation system is capable of dynamic system simulation and offers advantages such as high compatibility, interactivity, intuitive flexibility, and powerful graphics. It has been widely used in multi-platform and multidisciplinary application research. Unlike commercial CNC controllers, which use the current position measured by linear or rotary encoders to compensate for machine tool volumetric errors, the Matlab/Simulink platform compensates based on continuous time. This approach more effectively addresses the issue of intermittent compensation based on discrete position data, resulting in improved compensation performance and higher accuracy.

The development of a dynamic compensation model for machine tool volumetric errors within the Simulink environment involves three fundamental stages:

(1)Establishing an error fitting module based on measured data. The set of 21 geometric error parameters, obtained via laser interferometer measurements, is loaded into the MATLAB workspace to facilitate subsequent model construction. Use the Curve Fitting Toolbox to perform fitting with a quintic polynomial, generate continuous functions of each error term varying with position, and encapsulate the fitting results into a Subsystem module with parameter input to realize real-time calling of error curves.

(2) Building a time-position mapping and compensation calculation link. Integrate a Sine Wave module in the model to simulate the feed speed curve of each axis, convert the speed signal into a continuous position signal through an Integrator module, which serves as the input of the error fitting module. Meanwhile, based on the simplified formulas derived from the Abbe and Bryan principles, construct an error coupling calculation unit in the Math Operations module group. The volumetric error is synthesized by integrating the error components along the X, Y, and Z axes based on their spatial coupling relationships, and the computed real-time compensation is superimposed to produce the corrected position command.

(3) Constructing a closed-loop verification and visualization module. The corrected position command is routed to the Transfer Fcn block within Simulink's Continuous module library to simulate the servo system's dynamic response, and the resulting output yields the actual position signal. Real-time comparison of error curves before and after compensation is conducted through the Scope

module, and key data are exported to Matlab for quantitative analysis (such as maximum deviation, root mean square error, etc.) using the To Workspace module. The entire model adopts a modular design, with each functional unit connected by signal lines, supporting online parameter adjustment and dynamic simulation. Eventually, a complete closed-loop link from speed input to compensation output is formed, realizing dynamic correction of full-stroke errors based on continuous time.

3.2 Simulink modeling

To enable volumetric error compensation using the MATLAB/Simulink platform, the process begins with the acquisition of 21 geometric error parameters for each axis, measured across the machine's workspace. These data are then fitted in MATLAB to generate continuous error curves. When the machine tool traverses along the X, Y, and Z directions with feed rates V_x, V_y, and V_z, the corresponding displacement in each axis can be computed as follows:

$$\begin{cases} x = Vx \times t \\ y = Vy \times t \\ z = Vz \times t \end{cases} \tag{28}$$

The continuous-time compensation framework addressing quasi-static errors based on continuous time can be derived by determining the feed rate of each axis according to the actual machining conditions and applying the formulas from 1 to 28 in this study.

Accordingly, the integrated volumetric error model corresponding to the X-axis direction is illustrated in Fig. 5.

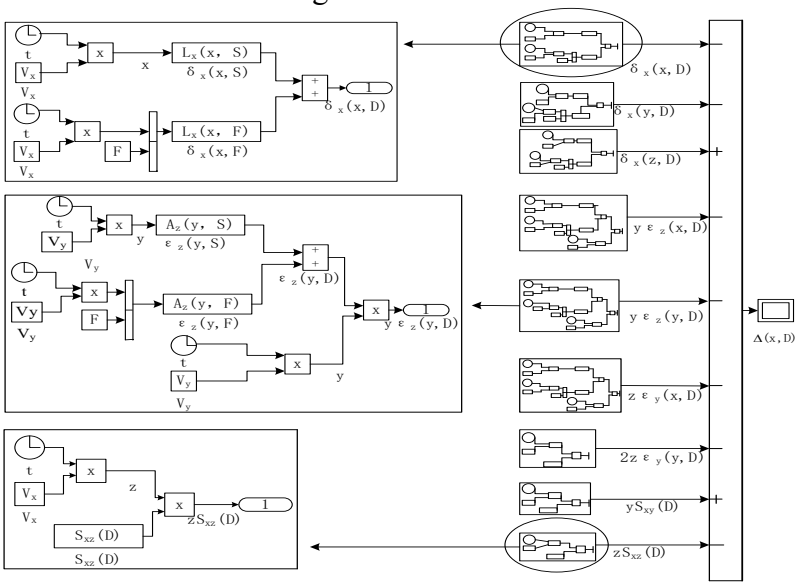

Fig.4. Integrated volume error compensation model for the X-axis

By applying an analogous approach, the volumetric error models for the Y- and Z-axes are established, as depicted in Figures 5 and 6.

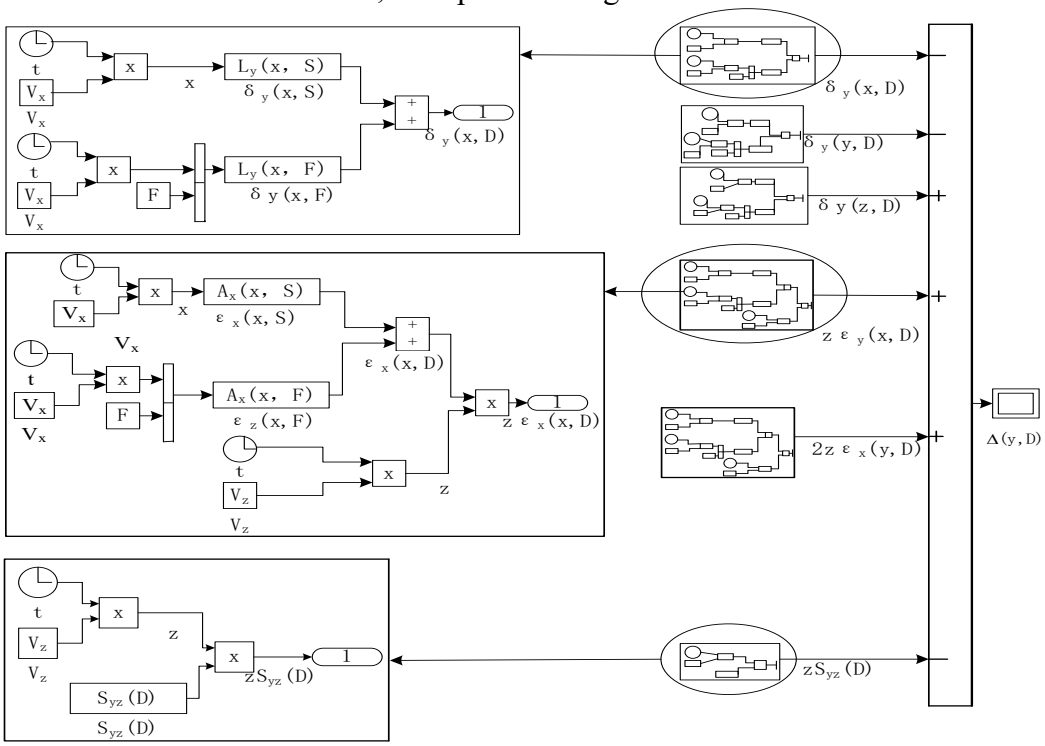

Fig. 5. Integrated volume error compensation model in Y-axis direction

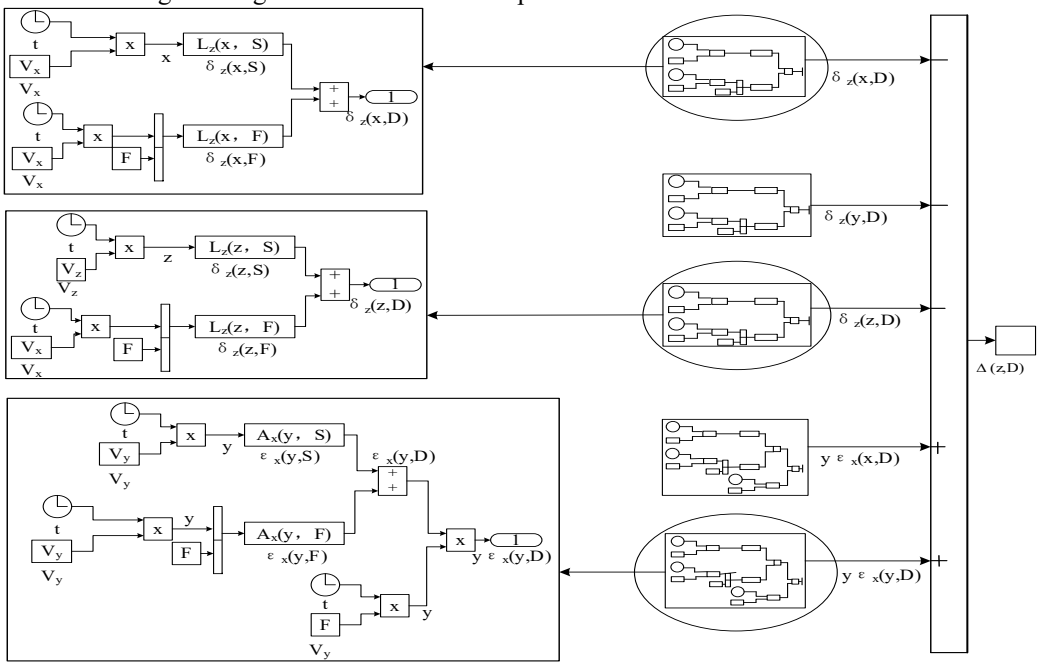

Fig. 6. Integrated volume error compensation model in Z-axis direction.

4 Application verification

The experimental investigation was conducted on the XHK715 vertical machining center, as illustrated in Fig. 7. The machine is equipped with travel ranges of 1800 mm (X-axis), 1500 mm (Y-axis), and 1200 mm (Z-axis), and features a worktable with dimensions of 500 mm in width and 1050 mm in length.

Fig. 7. XHK715 three-axis vertical machining center.

4.1 Measurement of Volumetric Machine Tool Errors

To ensure safe operation and reliable measurement conditions, the effective working ranges were set to −800 to 0 mm for the X-axis, −500 to 0 mm for the Y-axis, and −500 to 0 mm for the Z-axis. In accordance with applicable national metrology standards, a uniform measurement interval of 50 mm was adopted for the X, Y, and Z axes. A total of 17 measurement points were distributed along the X-axis, while 11 points were allocated along both the Y- and Z-axis directions to ensure sufficient spatial resolution. The angular, positional, and straightness errors of the Abbe point on each axis were measured sequentially using a laser interferometer, with the results presented in Figures 8, 9, and 10. The three squareness errors, measured using a laser interferometer, are as follows: $S_{xy} = 0.00148\text{mm/m}$, $S_{xz} = 0.00182\text{mm/m}$, and $S_{yz} = 0.00132\text{mm/m}$.

Where The measurement range of the X-axis spans from −800 mm to 0 mm, the measurement pitch is 50 mm, the angular error is -31.05 to 37.51 μm, the positioning error in the Abbe point ranges from 0.41 to 14.74 um, and the straightness error in the Abbe point is -25.91~0.98 μm.

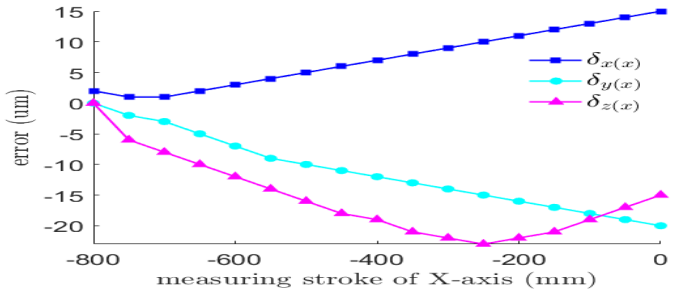

(a) Three Linear Geometric Error Components Along the X-Axis

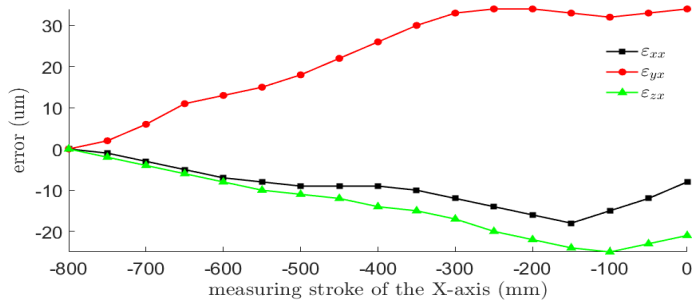

(b) Three Angular Geometric Error Components Along the X-Axis

Fig. 8 Measurement Results of Six Geometric Error Components Along the X-Axis

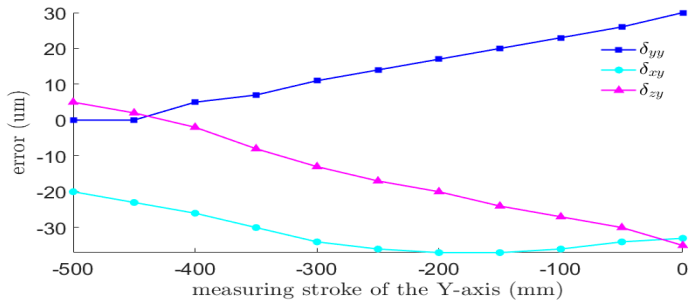

(a) 3-term linear geometric errors of Y-axis

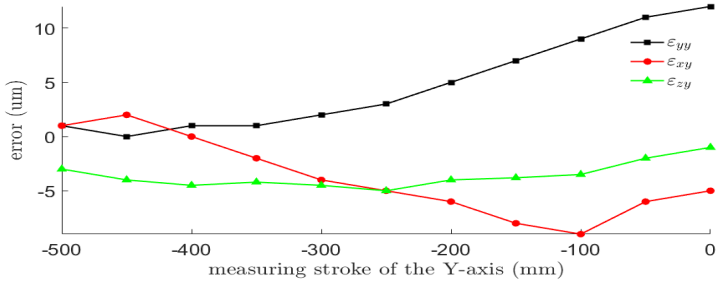

(b)3-term angular geometric errors of Y-axis

Fig. 9 Detecting results of six-term geometric errors of Y-axis.

The Y-axis was measured over a stroke range of −500 mm to 0 mm, with a measurement interval of 50 mm. Within this range, the angular error varied between −9.25 μm and 13.03 μm; the positioning error at the Abbe point ranged from −1.2 μm to 33.25 μm; and the straightness error at the Abbe point was observed to vary between −39.36 μm and 4.26 μm.

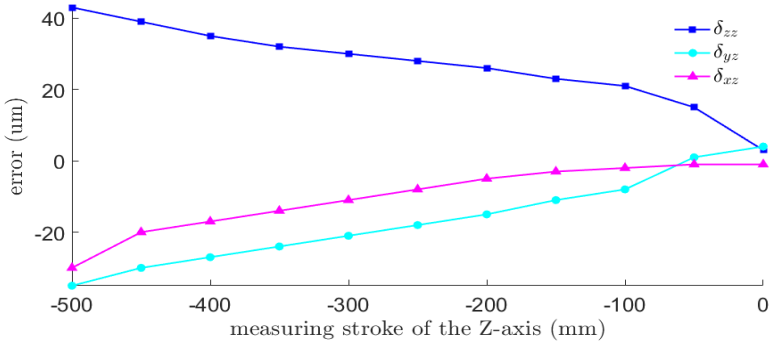

(a) 3-term linear geometric errors of Z-axis

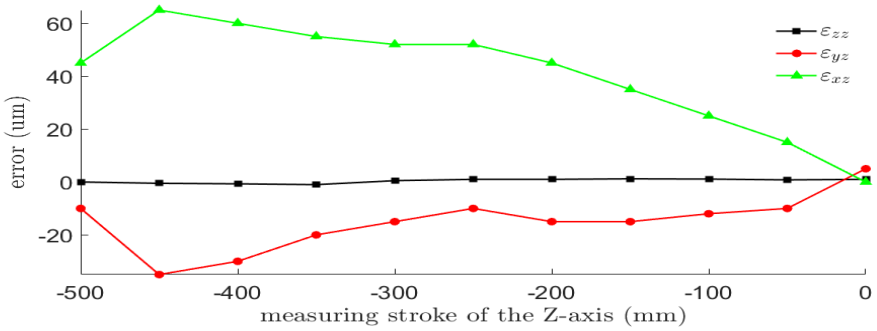

(b)3-term angular geometric errors of Z-axis

Fig. 10 Detecting results of six-term geometric errors of Z-axis.

For the Z-axis, measurements were conducted over a travel range of −500 mm to 0 mm with a spacing of 50 mm between sampling points. The observed angular error varied from −34.11 μm to 62.68 μm, the positioning error at the Abbe point ranged from 3.89 μm to 42.24 μm, and the corresponding straightness error ranged from −34.46 μm to 2.66 μm.

4.2 Error compensation

In this study, the geometric error data of the three translational axes were fitted using a fifth-order polynomial in MATLAB to generate continuous error curves for subsequent compensation modeling[14]. Additionally, considering the machine's potential and tool cutting performance, the feed speeds of the three moving axes were selected as $V_x = -0.035mm/s$, $V_y = -0.02mm/s$, $V_z = -0.02mm/s$ (where the negative sign indicates the direction of movement)

to achieve high quality, high productivity, low production cost, and safe operation. These parameters were then incorporated into the error compensation model described[15]. As illustrated in Fig.11, the model calculates real-time compensation values E_x,$E_y$and E_z based on the current operational time. These correction values are superimposed onto the corresponding real-time position coordinates x, y, and z, and the resulting signals are transmitted to the motor control system to mitigate quasi-static errors and enhance machining accuracy.

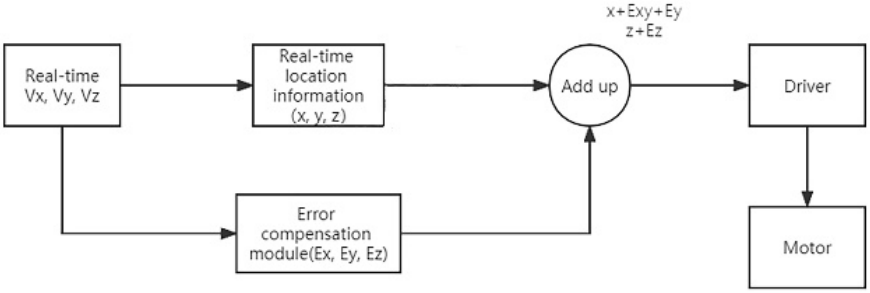

Fig. 11 Error compensation flowchart

To further substantiate the proposed approach, Table 2 presents a comparison between static and dynamic error compensation methods. The results indicate that dynamic compensation leads to markedly improved accuracy and greater consistency in machine tool performance.

Table 2

Comparison results between static error and dynamic error compensation

axis	error item	before compensation	static compensation	dynamic compensation
X-axis	positioning error(μm)	0.41~14.74	0.36~6.82	0.31~4.14
	straightness error (μm)	-25.91~ 0.98	-8.63~0.85	-5.26~0.78
	angular error(μrad)	-31.05~ 37.51	-15.27~12.98	-4.23~5.31
Y-axis	positioning error(μm)	-1.2 ~ 33.25	-0.46~9.80	-0.47~4.83
	straightness error(μm)	-39.36~4.26	-13.78~4.22	-6.11~2.60
	angular error(μrad)	-9.25 ~13.03	-5.40~6.35	-2.37~3.64
Z-axis	positioning error(μm)	3.89 ~ 42.24	1.89~13.49	1.80~5.66
	straightness error(μm)	-34.46 ~2.66	-10.29~2.22	4.68~2.20
	angular error(μrad)	-34.11~62.68	-14.32~16.69	-6.87~7.38

4.3 Evaluation of the machining effects on parts

To verify the machine tools' accuracy after compensation, an evaluation was conducted by machining parts. The machining was performed on an XHK715 3-axis vertical machining center, using a 60 cm × 60 cm × 20 cm rectangular block as the substitute machining part. The G-code for the machining program was edited based on the machining drawing. The machined surface was processed using an X12 milling cutter, with a spindle speed of 2000 r/min; the feed rates alogng the X-, Y-, and Z-axes were set to $\mathbf{V_x = -0.035mm/s}$, $\mathbf{V_y = -0.02mm/s}$,

$V_z = -0.02mm/s$, respectively, with a cutting depth of 2 mm. The corresponding machined components are shown in Fig. 12.

(a)Surface of the part before compensation (b)Surface of the part after compensation

Fig. 12 Comparison of machined parts.

Where (a) refers to the sample part machined by the machine tool before compensation; (b) represents the sample part machined after compensation using the method proposed in this study. It is evident that the former exhibits minor issues such as burrs and gaps, while the latter shows a smooth and flawless surface. To more accurately evaluate the quality of the machined parts with and without compensation, a Zeiss CMM was used to test the linear accuracy of the machined samples. The experimental results are presented in Fig. 13.

In Fig. 13(a), the results of the coordinate measurement used to evaluate the contour of the machined part prior to error compensation are presented; In Fig. 13(b), the three-coordinate measurement results after implementation of the proposed compensation strategy are shown, reflecting enhancements in geometric accuracy. According to the results of the CMM inspection, the linear profile deviation of the machined workpiece was reduced from 0.1677 mm prior to compensation to 0.0507 mm following the application of the proposed method, demonstrating a substantial enhancement in machining accuracy.

(a)result of three-coordinate measurement of the machined part before compensation

(b)result of three-coordinate measurement of the machined part before compensation

Fig. 13 Inspection chart of CMM.

4.4 Discussion

The comparative analysis of static and dynamic error compensation results and the CMM verification data demonstrate that the proposed continuous-time dynamic compensation method achieves significant improvements in both compensation accuracy and stability, outperforming traditional approaches in several key aspects.

Quantitatively, the dynamic compensation method exhibits a more pronounced reduction in error ranges compared to static compensation. For instance, the maximum positioning error of the X-axis is reduced by 72% (from 14.74 μm pre-compensation to 4.14 μm post-dynamic compensation), which is 38% higher than the improvement achieved by static compensation (which reduced the maximum positioning error to 6.82 μm, a 54% reduction). Similarly, the Z-axis angular error shows a 89% reduction (from 62.68 μrad to 7.38 μrad) under dynamic compensation, far exceeding the 74% reduction from static compensation. On average, dynamic compensation reduces the maximum values of positioning, straightness, and angular errors by 68%, 62%, and 75% respectively, while static compensation yields average reductions of 45%, 40%, and 52%—indicating that the proposed method improves precision by an additional 23–25% compared to static strategies.

In terms of overall machining accuracy, the linear profile deviation decreases from 0.1677 mm to 0.0507 mm, representing a 69.8% reduction. This improvement is quite significant, two reasons as follows: (1) the integration of Abbe and Bryan principles minimizes systematic measurement errors overlooked by traditional models, and (2) the continuous-time framework eliminates interpolation gaps in discrete compensation, ensuring real-time correction across the full stroke.

A potential limitation is that the current model focuses on quasi-static errors, and future work will incorporate thermal and load-induced dynamic errors to further broaden its applicability. Nonetheless, the quantitative comparisons confirm that the method offers a more robust and efficient solution for machine tool volumetric error compensation.

5 Conclusion

Compensation is an effective methods to enhance machine tools machining precision. Traditional volumetric error compensation modeling relies on discrete position coordinate information, where discontinuous compensation affects the overall effectiveness. This study presents a novel continuous-time dynamic compensation strategy for volumetric errors in machine tools, aiming to resolve the limitations associated with discontinuous compensation. The proposed method further incorporates the Abbe and Bryan principles into the error

modeling process, enhancing measurement fidelity and machining precision. The primary contributions of this work are summarized as follows:

(a) Based on the above two principles, the causes of Abbe and Bryan errors associated with machine tool detection were investigated. A compensation model for machine tool volumetric errors, including Abbe and Bryan errors, was established, and the model was simplified by converting the Bryan point to the Abbe point.

(b) Matlab software was utilized to fit the geometric error data obtained from measurements, and a continuous-time model for dynamic compensation of machine tool volumetric errors was developed using the Matlab/Simulink module.

(c) The parts were machined on an XHK715 3-axis vertical machining center for verification. Its effectiveness was validated by comparing the machined parts before compensation with those after compensation using the method described in this study.

This study offers two primary advantages. First, by integrating the Abbe and Bryan principles into the modeling framework and unifying the Abbe and Bryan reference points, the proposed method simplifies the volumetric error compensation model and lowers the computational burden on the CNC system. Second, the use of the Matlab/Simulink module enables volumetric error dynamic compensation for machine tools, addressing the traditional issue of discontinuous compensation based on discrete coordinate positions. In addition, the present study primarily addresses the modeling of volumetric errors in machine tools operating under quasi-static or unloaded conditions. However, factors affecting the machine's machining precision also include thermal effects, loads, load variations, and other dynamic errors. Therefore, this study is limited in scope, and future research should consider additional influencing factors.

Acknowledgement

The authors gratefully acknowledge the financial support provided by the 2022 Joint Fund for Innovation and Development of Hubei Natural Science Foundation (Grant No. 2022CFD081) and the Hubei Provincial Support for Enterprise Technological Innovation and Development Project in 2022 (2022BAD099) and Hubei Provincial Department of Education Scientific Research Project in 2023(B2023480).

REFERENCES

[1] *Xia HJ, Peng WC, Ouyang XB, Chen XD, Wang SJ, Chen X*. Identification of geometric errors of rotary axis on multi-axis machine tool based on kinematic analysis method using double ball bar[J].International Journal of Machine Tools and Manufacture, **vol.122**, Nov. 2017, pp. 161-175

[2] *Tianci F, Cui CJ, Shan W, Dong DF, Zhou WH, Li JL*. A study on the real-time compensation system based on Abbe principle for range accuracy of submicron measuring instrument[J].Measurement Science and Technology, **vol.33**, no. 8, May. 2022, pp. 188-203

[3] *Jie C.* Study on Full Error Model and Error Compensation Technology of CNC Machine Tool Based on Fold Dijkstra Algorithm//2021 13th International Conference on Measuring Technology and Mechatronics Automation (ICMTMA). IEEE, Jan. 2021, pp. 131-134

[4] *Ankit Agarwal, K.A. Desai*.Predictive framework for cutting force induced cylindricity error estimation in end milling of thin-walled components[J].Precision Engineering, **vol.66**, Jan. 2020, pp.209-219

[5] *Maeng S, Min S*. Simultaneous geometric error identification of rotary axis and tool setting in an ultra-precision 5-axis machine tool using on-machine measurement[J] Precision Engineering, **vol.63**, May. 2020, pp. 94-104

[6] *Li Z, Feng W, Yang J, et al.* An investigation on modeling and compensation of synthetic geometric errors on large machine tools based on moving least squares method[J]. Proceedings of the Institution of Mechanical Engineers, Part B: Journal of Engineering Manufacture, **vol.232**, no. 3, Feb. 2018, pp 412-427

[7] *Yuchao F, Yubin H, Yejin C, et al.* Fast volumetric error assessment of a gantry-type machine using multi-degree-of-freedom laser-based sensors and Vector Transfer Model[J]. The International Journal of Advanced Manufacturing Technology, **vol.118**, no. 11-12, Oct. 2021, pp 3711-3724

[8] *Oh JY, Choi SJ, Kim CJ, et al.* Estimation and compensation of cutting force induced position error in robot machining system[J]. Precision Engineering, **vol.86**, Dec. 2024, pp 101-108

[9] *Patil R.A., Gombi S.L*. Operational Cutting Force Identification in End Milling Using Inverse Technique to Predict the Fatigue Tool Life[J]. Iranian Journal of Science and Technology, Transactions of Mechanical Engineering, **vol.46**, Aug. 2022, pp. 31-41

[10] *Nguyen V H, Le T T, Truong H S, et al.* Predicting volumetric error compensation for five-axis machine tool using machine learning[J]. International Journal of Computer Integrated Manufacturing, **vol.36**, no. 8, Aug. 2023, pp. 1191-1218

[11] *Mayr J, Jedrzejewski J, Uhlmann E, Alkan Donmez M, Knapp W, Härtig F, Wendt K, Moriwaki T, Shore P, Schmitt R, Brecher C, Würz T, Wegener K*. Thermal issues in machine tools [J].CIRP Annals - Manufacturing Technology, **vol.61**, no. 2, Jun. 2012, pp. 771-791

[12] *Gregory W. Vogl, Dominique A.* Regli, Gregory M. Corson. Real-time estimation of cutting forces via physics-inspired data-driven model[J].CIRP Annals - Manufacturing Technology, **vol.71**, no. 1, Jan. 2022, pp. 317-320

[13] *Lahmiri, S., Tadj, C., Gargour, C., et al.* Optimal tuning of support vector machines and k-NN algorithm by using Bayesian optimization for newborn cry signal diagnosis based on audio signal processing features[J].Chaos, Solitons and Fractals: the interdisciplinary journal of Nonlinear Science, and Nonequilibrium and Complex Phenomena, **vol.167**, Dec. 2023, 167(112972),pp. 1-6

[14] *Gao W, Weng L, Zhang J, et al.* An improved machine tool volumetric error compensation method based on linear and squareness error correction method[J]. The International Journal of Advanced Manufacturing Technology, **vol.106**, no. 11-12, Feb. 2020, pp. 4731-4744
[15] *Zhu Zerun, PENG Fangyu, YAN Rong, et al.* Influence mechanism of machining angles on force induced error and their selection in five axis bullnose end milling[J]. Chinese Journal of Aeronautics, **vol.33**, no. 12, Apr. 2020, pp. 3447-3459